



Evidence for rigid triaxial deformation at low energy in ^{76}Ge

Y. Toh,^{1,2} C. J. Chiara,^{2,3} E. A. McCutchan,^{2,4} W. B. Walters,³ R. V. F. Janssens,² M. P. Carpenter,² S. Zhu,² R. Broda,⁵ B. Fornal,⁵ B. P. Kay,² F. G. Kondev,⁶ W. Królas,⁵ T. Lauritsen,² C. J. Lister,^{2,*} T. Pawlat,⁵ D. Seweryniak,² I. Stefanescu,^{2,3} N. J. Stone,^{7,8} J. Wrzesiński,⁵ K. Higashiyama,⁹ and N. Yoshinaga¹⁰

¹Japan Atomic Energy Agency, Tokai, Ibaraki 319-1195, Japan

²Physics Division, Argonne National Laboratory, Argonne, Illinois 60439, USA

³Department of Chemistry and Biochemistry, University of Maryland, College Park, Maryland 20742, USA

⁴National Nuclear Data Center, Brookhaven National Laboratory, Upton, New York 11973-5000, USA

⁵Niewodniczański Institute of Nuclear Physics PAN, PL-31-342, Kraków, Poland

⁶Nuclear Engineering Division, Argonne National Laboratory, Argonne, Illinois 60439, USA

⁷Department of Physics, University of Oxford, OX1 3PU Oxford, United Kingdom

⁸Department of Physics and Astronomy, University of Tennessee, Knoxville, Tennessee 37996, USA

⁹Department of Physics, Chiba Institute of Technology, Narashino, Chiba 275-0023, Japan

¹⁰Department of Physics, Saitama University, Saitama City 338-8570, Japan

(Received 10 January 2013; published 11 April 2013)

Excited states of ^{76}Ge have been populated in above-barrier Coulomb excitation and inelastic scattering of a 530-MeV ^{76}Ge beam on a ^{238}U target and studied using in-beam γ -ray spectroscopy with the Gammasphere array. The γ band was extended considerably and one new band was identified. Comparisons of the γ band with collective- and shell-model calculations suggest that ^{76}Ge may be a rare example of a nucleus exhibiting rigid triaxial deformation in the low-lying states.

DOI: [10.1103/PhysRevC.87.041304](https://doi.org/10.1103/PhysRevC.87.041304)

PACS number(s): 23.20.Lv, 23.20.En, 21.60.Ev, 27.50.+e

Triaxial deformation has been a subject of much interest in the study of nuclear structure. While static triaxial deformation has been firmly established at high spin, see, e.g., Refs. [1–4], it remains an open question as to whether nuclei can exhibit rigid triaxiality in their low-lying structure. There are two simple models to describe deviations from axial symmetry within the framework of the Bohr Hamiltonian [5]. The rigid triaxial model of Davydov and Filippov (DF) [6] has a well-defined potential minimum at a nonzero value of γ , whereas the γ -soft model of Wilets and Jean (WJ) [7] considers a potential that is completely flat in the γ degree of freedom. Both of these models have similar predictions for level energies in the ground-state band and for $B(E2)$ transition strengths. One defining signature is in the energies of the levels making up the γ band. In the γ -soft model, the energies are grouped such that the states with odd spin I are closer in energy to the $I + 1$ even-spin states than to those with spin $I - 1$, i.e., they exhibit a 2^+ , $(3^+, 4^+)$, $(5^+, 6^+)$, ... grouping. This is in contrast to the DF model pattern of $(2^+, 3^+)$, $(4^+, 5^+)$, $(6^+, 7^+)$, ... Therefore, the staggering of the odd- and even-spin levels of a γ band can be viewed as an important structural indicator [8].

Low-lying structures of Ge isotopes have been the subject of a large number of experimental studies involving in-beam γ -ray spectroscopy [9–12]. However, there has been little available experimental information on the γ bands in Ge isotopes in the spin range of interest. Chou *et al.* [13] have suggested that the even-even Ge isotopes with $A = 72 - 78$ exhibit the characteristics of an asymmetric rotor with $\gamma \sim 30^\circ$, but they had insufficient experimental evidence to

distinguish between a γ -soft or γ -rigid asymmetry. In a more global investigation, Ref. [14] used the sum-rule method to calculate the eccentricity of even-even nuclei with $46 \leq A \leq 192$, $22 \leq Z \leq 76$. They found that, of about 70 nuclei with sufficient $B(E2)$ information, only $^{72,74,76}\text{Ge}$ and $^{74,76,78}\text{Se}$ showed pronounced asymmetry compared to surrounding nuclei. Their analysis in terms of third-order products of $B(E2)$ strengths also could not be used to determine whether the triaxiality is soft or rigid. From a purely theoretical standpoint, recent Hartree-Fock microscopic calculations [15] using a variety of forces have predicted low-lying triaxial shapes in ^{76}Ge with $\gamma \sim 21 - 26^\circ$.

In the present work, we report on an experimental study of the level scheme of ^{76}Ge aimed at addressing the open question of the low-lying structure of this nucleus. Using both above-barrier Coulomb excitation and inelastic scattering, non-yrast levels in ^{76}Ge were populated up to moderate spin ($I_{\text{max}} \sim 12\hbar$). A number of bands were newly identified or extended in this way, in particular the γ band, the properties of which can shed light on the shape of ^{76}Ge at low-spin.

A 530-MeV ^{76}Ge beam from the Argonne Tandem Linear Accelerator System (ATLAS) at Argonne National Laboratory bombarded a ^{238}U target to populate excited states in ^{76}Ge . The target thickness was ~ 55 mg/cm², sufficient to stop all reaction products. Emitted γ rays were detected by the Gammasphere array, which consisted of 100 Compton-suppressed HPGe detectors arranged in 16 rings relative to the beam axis [16,17]. The beam energy corresponds to a value about 33% above the Coulomb barrier. Therefore, excited levels in ^{76}Ge were populated not only through Coulomb excitation, but also in inelastic-scattering reactions. The trigger condition required three or more Compton-suppressed γ rays to be present in prompt coincidence. A total of 2.8×10^9 such

*Present address: Department of Physics, University of Massachusetts, Lowell, Massachusetts 01854, USA.

coincidence events were collected during a four-day run with an average beam intensity of about 0.1 pnA.

The data were sorted into a three-dimensional histogram of γ -ray energies ($\gamma\gamma\gamma$ cube) for level-scheme construction based on observed coincidence relationships. A time cut was placed such that only those γ rays recorded within a ~ 40 -ns time window centered on the prompt beam burst were selected. A second, delayed- γ cube was created with a γ -ray time cut placed to select only those transitions falling in the time interval between beam bursts. The prompt and delayed cubes could be analyzed for coincidence events from the beam-induced reactions or from β and isomeric γ decays, respectively. For γ -ray angular-correlation (AC) measurements, a set of 12 two-dimensional histograms ($\gamma\gamma$ matrices) was also sorted, with each matrix covering a particular range of relative angles between pairs of detectors, following the method outlined in Ref. [18]. The analysis of the cubes and the matrices was performed using the RADWARE analysis package [19].

The partial level scheme of ^{76}Ge deduced from the prompt coincidence cube is given in Fig. 1. Properties of the ^{76}Ge level scheme deduced from the prompt data are given in Table I. Since excited levels in ^{76}Ge were populated in both Coulomb-excitation and inelastic-scattering reactions, γ -ray intensities are given only as relative branchings from each level. The following discussion focuses on the levels presented in Fig. 1, however, additional levels and γ rays were observed and their properties can be found in Table I.

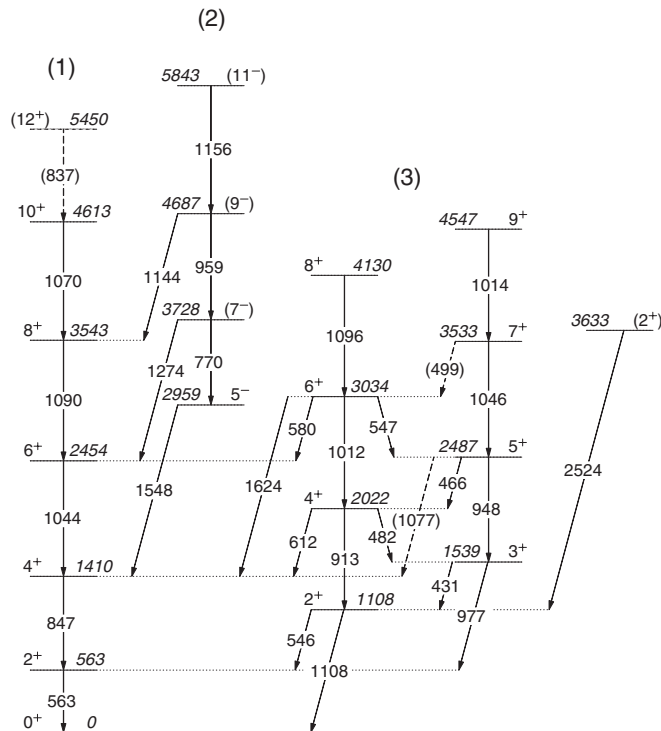


FIG. 1. Partial level scheme of ^{76}Ge deduced from the prompt data in this work. Level and transition energies are given in keV. Only those states relevant to the discussion are shown; all are given in Table I.

TABLE I. Excitation energies E_{lev} , γ -ray energies E_{γ} , branching ratios BR , mixing ratios δ , and spin-parity assignments $I_i^{\pi} \rightarrow I_f^{\pi}$ of initial and final states for γ rays placed in ^{76}Ge from the prompt data. Not all states are shown in Fig. 1.

E_{lev} (keV)	E_{γ} (keV)	BR	$\delta(E2/M1)$	$I_i^{\pi} \rightarrow I_f^{\pi}$
562.9	562.9(1)	100		$2_1^+ \rightarrow 0_1^+$
1108.4	545.5(3)	100	+2.1(4)	$2_2^+ \rightarrow 2_1^+$
	1108.4(3)	75(8)		$2_2^+ \rightarrow 0_1^+$
1410.1	847.2(4)	100		$4_1^+ \rightarrow 2_1^+$
1539.5	431.0(3)	65(7)	+1.8(4)	$3_1^+ \rightarrow 2_2^+$
	976.5(3)	100	+2.5(2)	$3_1^+ \rightarrow 2_1^+$
			or +0.37(8)	
			+0.23(4)	
2021.7	482.2(6)	15(8)		$4_2^+ \rightarrow 3_1^+$
	611.6(4)	85(15)	+0.50(8)	$4_2^+ \rightarrow 4_1^+$
	913.2(4)	100		$4_2^+ \rightarrow 2_2^+$
2453.8	1043.7(3)	100		$6_1^+ \rightarrow 4_1^+$
2487.3	465.6(4)	10(8)		$5_1^+ \rightarrow 4_2^+$
	947.8(4)	100		$5_1^+ \rightarrow 3_1^+$
	(1077.2(4))	5(5)		$5_1^+ \rightarrow 4_1^+$
2669.2	647.5(4)	21(3)		$\rightarrow 4_2^+$
	1129.7(4)	100		$\rightarrow 3_1^+$
	1259.1(4)	59(6)		$\rightarrow 4_1^+$
2733.4	1193.9(4)	90(20)		$4_3^+ \rightarrow 3_1^+$
	1625.0(4)	100		$4_3^+ \rightarrow 2_2^+$
2958.6	1548.5(4)	100	+0.0(4)	$5^- \rightarrow 4_1^+$
2988.2	319.0(3)	100		
	500.9(4)	8(3)		$\rightarrow 5_1^+$
	534.4(4)	25(10)		$\rightarrow 6_1^+$
3033.9	546.6(4)	20(20)		$6_2^+ \rightarrow 5_1^+$
	580.1(4)	60(15)	+1(4)	$6_2^+ \rightarrow 6_1^+$
	1012.2(4)	100		$6_2^+ \rightarrow 4_2^+$
	1623.8(4)	40(15)		$6_2^+ \rightarrow 4_1^+$
3235.9	782.1(4)	100		$(6_3^+) \rightarrow 6_1^+$
	1825.8(4)	40(30)		$(6_3^+) \rightarrow 4_1^+$
3437.0	767.8(4)	100		
3533.0	(499.1(4))	20(20)		$7_1^+ \rightarrow 6_2^+$
	1045.7(4)	100		$7_1^+ \rightarrow 5_1^+$
3536.1	547.9(4)	100		
3543.4	1089.6(4)	100		$8_1^+ \rightarrow 6_1^+$
3632.8 ^a	2524.4(4) ^a	100		$(2_3^-) \rightarrow 2_2^+$
3728.1	769.5(4)	30(20)		$(7^-) \rightarrow 5^-$
	1274.3(4)	100	+9(7)	$(7^-) \rightarrow 6_1^+$
			or +0.2(6)	
3783.9	750.0(4)	100		$\rightarrow 6_2^+$
	825.3(4)	25(20)		$\rightarrow 5^-$
4129.9	1096.0(4)	100		$8_2^+ \rightarrow 6_2^+$
4130.5	894.6(4)	100		$\rightarrow (6_3^+)$
4311.2	775.1(4)	70(20)		
	1323.0(4)	100		
4547.0	1014.0(4)	100		$9_1^+ \rightarrow 7_1^+$
4613.1	1069.7(4)	100		$10_1^+ \rightarrow 8_1^+$
4687.0	958.9(4)	100		$(9^-) \rightarrow (7^-)$
	1143.6(4)	40(30)		$(9^-) \rightarrow 8_1^+$
4720.8	936.9(4)	100		$\rightarrow (7_2^+)$
	(992.7(4))	5(5)		$\rightarrow (7^-)$
5450.1	(837.0(4))	100		$(12_1^+) \rightarrow 10_1^+$
5843.4	1156.4(4)	100		$(11^-) \rightarrow (9^-)$

^aObserved in delayed data and very weakly in prompt data.

The levels and γ rays observed in Ref. [20] were confirmed in the present experiment. These results extend the ground-state band (band 1) up to a 10^+ state at 4613.1 keV, with a tentatively proposed 12^+ state at 5450.1 keV. Spin and parity assignments are supported by the AC measurements.

Band 2 is newly observed in this work. This sequence feeds the ground-state band via 1548.5-, 1274.3-, and 1143.6-keV γ rays, which have ACs consistent with stretched-dipole multipolarity. The state at 2958.6 keV is likely the same as the one at 2957(5) keV observed with $L = 5$ transfer in the (t, p) reaction of Ref. [21]. We, therefore, assign $I^\pi = 5^-$ to this level and tentatively up to (11^-) for the 5843.4-keV state.

This paper focuses on the newly developed γ band, labeled 3 in Fig. 1. The levels at 1108.4 keV and 1539.5 keV reported in Ref. [22] have been confirmed. The spin and parity assignment of 2^+ to the 1108.4-keV state, as assigned in Ref. [10], is confirmed in this work by the AC measurement of the 562.9-545.5-keV cascade (using the well-established pure $E2$ character for the $2_1^+ \rightarrow 0_1^+$, 562.9-keV transition). The $\delta(E2/M1)$ mixing ratio for the 545.5-keV transition to the 2_1^+ state is determined to be $\delta = +2.1(4)$ [$A_2 = -0.30(1)$, $A_4 = 0.27(2)$], consistent with the evaluated value [$+3.5(15)$]. For the AC analysis of the data for the 976.5-keV, $3_1^+ \rightarrow 2_1^+$ γ ray, two solutions were obtained in this work, $\delta(E2/M1) = +2.5(2)$ [$A_2 = 0.09(2)$, $A_4 = -0.07(1)$] or, less likely, $+0.23(4)$ [$A_2 = 0.09(2)$, $A_4 = -0.004(4)$]. The adopted mixing ratio in Ref. [10] is $\delta(E2/M1) = +2.0_{-3}^{+5}$ or $+0.75_{-10}^{+15}$. For the 431.0-1108.4-keV cascade, two possible values for $\delta(E2/M1)$ were obtained, $+1.8(4)$ [$A_2 = 0.16(5)$, $A_4 = -0.06(1)$] or, less likely, $+0.37(8)$ [$A_2 = 0.17(4)$, $A_4 = -0.010(4)$]; there are no previous experimental data available for comparison. Thus, spin and parity are firmly established for the 2^+ and 3^+ levels in band 3.

In our prompt data set, we observe a 913.2(4)-keV transition decaying from a level at 2021.7 keV to the known 2_2^+ state. This is consistent with the 913.2(5)-keV decay identified in an $(n, n'\gamma)$ reaction from a state at 2021.7(6) keV [10]. A similar, but inconsistent, 911.40(10)-keV γ ray was identified in the γ -ray-singles spectrum following β decay of ^{76}Ga , and placed as depopulating a state at 2019.87(10) keV [22]. The evaluation of Ref. [10] adopted the latter transition energy, and assigned tentative $I^\pi = (4^+)$ based on observed $L = (4)$ transfer in (t, p) [21] and (p, p') [23] reactions to a level at around 2020 keV [2017(5) and 2022(5) keV, respectively].

As our reaction also produces ^{76}Ga , the apparent discrepancy in the transition and level energies can be addressed by considering the delayed- γ subset of our data. In Ref. [22], a 3632.75-keV (2^+) state populated in the β decay of ^{76}Ga was reported to decay via a 1612.7-911.4-545.5-562.9-keV γ -ray cascade, passing through the proposed level at 2019.87 keV mentioned above. Double gating on the 562.9- and 545.5-keV transitions in our delayed cube showed no evidence for peaks at 911.4 or 1612.7 keV from the cascade reported in Ref. [22]. The 3632.8-keV level is confirmed, however, through observation of a depopulating 2524.4-keV transition (Fig. 1); a γ ray with this energy was similarly placed in Ref. [22]. Based on the relative intensities quoted in Ref. [22] for the 2524.4- and 1612.7-keV γ rays, the latter would have been observable here. In the same spectrum, a 913.2-keV

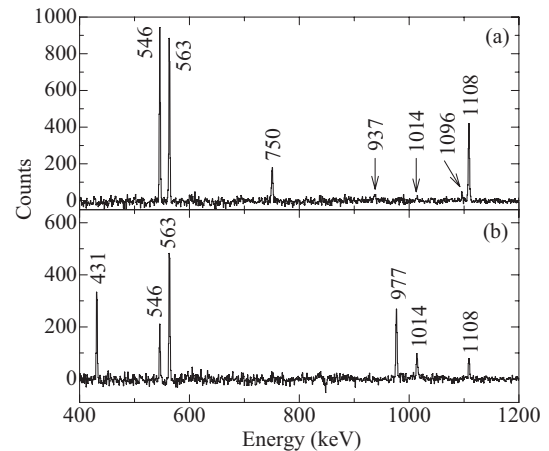


FIG. 2. Background-subtracted spectra double gated on (a) the 913- and 1012-keV transitions, and (b) the 948- and 1046-keV transitions in ^{76}Ge .

transition is observed instead of one at 911.4 keV. This is the γ ray that was placed decaying out of the 2021.7-keV state from the prompt cube (Fig. 1) and from $(n, n'\gamma)$ [10]. Thus, the present results confirm the existence of a state at 3632.8 keV, as well as one at 2021.7 keV (913.2-keV decay) rather than 2019.9 keV (911.4-keV decay). The ~ 2020 -keV (4^+) state identified in the (t, p) and (p, p') studies then corresponds to the former, which we firmly assign as 4^+ .

Above the 2021.7-keV state, five additional levels up to 4547.0 keV have been added to band 3. As examples, the coincidence spectra double gated on the 913.2- and 1012.2-keV γ rays and on the 947.8- and 1045.7-keV γ rays, displayed in Fig. 2, led to the identification of the 1096.0- and 1014.0-keV transitions in the γ band. The 482.2-, 465.6-, and 546.6-keV intraband transitions were identified in extensive analysis of the prompt cube; the 499.1-keV and 1077.2-keV transitions have been tentatively placed. AC measurements up to the 3533.0-keV level and organization of these levels into a band suggest I^π assignments up to 9^+ for the 4547.0-keV state. Additionally, the lack of observation of the 1539.5- and 2487.3-keV levels in the (t, p) transfer reaction [21] is consistent with these being unnatural-parity 3^+ and 5^+ states.

As discussed above, it is difficult to distinguish between γ -soft and γ -rigid structure using basic observables of the low-lying states. For example, the $R_{4/2} = E(4_1^+)/E(2_1^+)$ ratio in ^{76}Ge of 2.51 is close to that of the γ -soft model, $R_{4/2} = 2.50$, as well as that of the DF model, $R_{4/2} = 2.67$ for $\gamma = 30^\circ$. Similarly, the $B(E2)$ ratio, $B(E2; 2_2^+ \rightarrow 0_1^+)/B(E2; 2_2^+ \rightarrow 2_1^+)$, is zero in both the γ -soft and γ -rigid models, and found to be very small experimentally in ^{76}Ge , $B(E2; 2_2^+ \rightarrow 0_1^+)/B(E2; 2_2^+ \rightarrow 2_1^+) = 0.027(3)$. However, the staggering parameter

$$S(I) = \frac{[E(I) - E(I-1)] - [E(I-1) - E(I-2)]}{E(2_1^+)}, \quad (1)$$

which quantifies how adjacent levels within a γ band are grouped, can be used to distinguish between γ -rigid and γ -soft potentials based on its phase [8]. For rigid triaxial potentials,

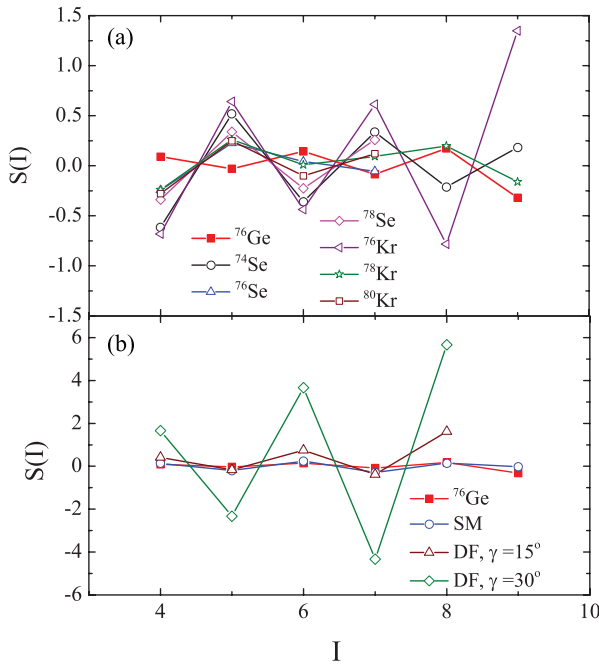


FIG. 3. (Color online) (a) Experimental staggering $S(I)$ for isotopes of Ge, Se, and Kr. (b) Experimental staggering in ^{76}Ge compared to the SM and DF-model predictions.

$S(I)$ exhibits an oscillating behavior that takes on high values for even spins and low values for odd spins, with the amplitude of the oscillation increasing with spin. The opposite phase exists for a γ -soft potential. The staggering of the γ band in ^{76}Ge is plotted as a function of spin in Fig. 3(a) in comparison with those for several neighboring Se and Kr isotopes. It is immediately clear that the staggering for ^{76}Ge follows the pattern of phase and increasing amplitude expected for a rigid triaxial shape, while all of the Se and Kr nuclei plotted have the opposite phase, namely that of a γ -soft potential. The γ bands are not well developed in $^{70,72,74}\text{Ge}$ —known only to the 4^+ state—but the value of $S(4)$ is negative for these and the Se and Kr nuclei, while ^{76}Ge has $S(4) > 0$. The sign of $S(4)$ was discussed in detail in Ref. [24] as being a strong indicator of the nature of the γ degree of freedom. Furthermore, as indicated by recent broad surveys of γ bands in medium-heavy mass nuclei, rigid triaxial nuclei are considerably scarcer than those that are γ -soft, see, e.g., Fig. 4 in Ref. [24] and Figs. 2–4 in Ref. [25]. Thus, ^{76}Ge appears to be the lone instance of a nucleus with a rigid triaxial shape in this region, and, more generally, is one of the rare known cases overall.

The experimental $S(I)$ values for ^{76}Ge are compared in Fig. 3(b) with predictions using the DF γ -rigid model with $\gamma = 15^\circ$ and 30° . As noted above, the phase of the $S(I)$ data for ^{76}Ge matches that predicted by the DF model. However, the amplitude of the observed staggering is significantly less than the calculated values. For the five cases identified in Ref. [24] as having an $S(I)$ phase consistent with DF (with spins extending up to at least $I = 8$), the overall magnitude of $S(I)$ was < 1.0 , again significantly smaller than the DF-model predictions for $\gamma = 30^\circ$. While it is possible to reduce the staggering amplitude by decreasing γ , doing so pushes the γ

band higher in excitation energy. Specifically, for $\gamma = 30^\circ$ the ratio of the energies of the two lowest 2^+ states is $E(2_2^+)/E(2_1^+) = 2.0$; by $\gamma = 15^\circ$, this ratio already reaches 6.9. The experimental value of 2.0 in ^{76}Ge suggests that the shape is near maximum triaxiality with $\gamma \approx 30^\circ$.

An alternative scenario that could produce a DF-like staggering pattern is if there is mixing between the ground-state and γ bands pushing the even-spin states of the latter higher in energy. With substantial mixing, a band with a γ -soft staggering pattern could be perturbed enough that the staggering resembles that of a γ -rigid nucleus. In ^{76}Ge , for the unperturbed states to have a staggering phase opposite that observed requires a large mixing matrix element of $V > 145$ keV, with corresponding unperturbed $E(2_2^+)/E(2_1^+)$ ratio below ~ 1.75 ; a staggering pattern similar to those of the neighboring Se and Kr isotopes requires an even larger $V > 200$ keV and ratio of 1.55 or less. Such a low energy for the 2_2^+ level would be difficult to explain with any collective model, which all give an $E(2_2^+)/E(2_1^+)$ ratio of 2.0 or larger. In addition, while large mixing matrix elements have been deduced in the classic examples of shape coexistence [26] involving the ground-state band and an intruder 0^+ band, such large mixing has not been previously observed between the ground band and the γ band. Thus, as both V and the $E(2_2^+)/E(2_1^+)$ ratio take on unrealistic values, band mixing is unlikely to be the origin of the inverted staggering compared to the neighboring nuclei.

In Table II, the ratios of $B(E2)$ transition strengths, $R = B(E2; I_i^\pi \rightarrow I_{f1}^\pi)/B(E2; I_i^\pi \rightarrow I_{f2}^\pi)$, are given for the experimental values (R_{exp}) and compared to the DF-model predictions (R_{DF}) for several states of the γ band. For the 2^+ , 3^+ , and 6^+ initial levels, R_{exp} is rather small, in agreement with the DF model, which predicts these particular ratios to be identically zero. Although not listed in the table, the ratio $B(E2; 4_2^+ \rightarrow 2_1^+)/B(E2; 4_2^+ \rightarrow 2_2^+)$ is comparably small, as no 1459-keV $4_2^+ \rightarrow 2_1^+$ transition was observed in the present data; this is also consistent with the expected ratio $R_{\text{DF}} = 0$. For the two levels with nonzero values, the DF model underestimates $R(4_2^+)$ by about a factor of three, while the prediction for $R(5_1^+)$ is consistent with the data, albeit only at

TABLE II. Ratios of $B(E2)$ rates between states with initial spin-parity I_i^π and final I_{f1}^π and I_{f2}^π , given by $R = B(E2; I_i^\pi \rightarrow I_{f1}^\pi)/B(E2; I_i^\pi \rightarrow I_{f2}^\pi)$. Experimental (exp) values are compared with those calculated by the DF (with $\gamma = 30^\circ$) and SM models. The first column gives the measured level energies in keV.

E_{exp}	I_i^π	I_{f1}^π	I_{f2}^π	R_{exp}	R_{DF}	R_{SM}
1108	2_2^+	0_1^+	2_1^+	0.027(3)	0	0.045
1539	3_1^+	2_1^+	2_2^+	0.029(+6) ₋₄ ^a	0	0.064
2022	4_2^+	4_1^+	2_2^+	1.3(4)	0.46	0.93
2487	5_1^+	4_2^+	3_1^+	< 6.3 ^b	1.00	1.29
3034	6_2^+	4_1^+	4_2^+	0.038(14)	0	0.48

^aRatio for the favored values of δ , +2.5(2) and +1.8(4) for the 977- and 431-keV transitions, respectively. If one or both of the less favored mixing ratios are used, R_{exp} lies within a range of about 0.001 to 0.3.

^bUpper limit assuming pure $E2$ character for the $5_1^+ \rightarrow 4_2^+$ transition.

the level of an upper limit. As noted in the introduction, the WJ γ -soft model predicts $B(E2)$ values similar to those of the DF model.

Overall, the DF model reproduces the γ band in ^{76}Ge fairly well: the calculated $E(2_2^+)/E(2_1^+)$ ratio, the sign (but not the magnitude) of the staggering $S(I)$, and the $B(E2)$ ratios are in reasonable agreement with the data, pointing towards a rigid shape with nearly maximal triaxiality ($\gamma \approx 30^\circ$) for ^{76}Ge . This model is somewhat of an oversimplified approach, however, so it is worth considering a more realistic one. Shell-model (SM) calculations were carried out to obtain level energies and $B(E2)$ ratios using the pairing-plus-quadrupole-type interaction. The $g_{9/2}$, $p_{1/2}$, $p_{3/2}$, and $f_{5/2}$ single-particle orbitals were taken into account for both neutrons and protons. The detailed prescriptions for the SM calculations are given in Ref. [27]. As is apparent from Fig. 3(b), the SM calculations reproduce not only the sign, but also the magnitude of the staggering much more closely than the DF calculations do. In addition, the energy of the γ bandhead is reproduced almost exactly, with the SM predicting $E(2_2^+)/E(2_1^+) = 2.0$. Absolute $B(E2)$ transition strengths can provide a consistency check that the 2_2^+ level in the SM calculations corresponds to the 2^+ level being considered as the γ bandhead. In experiment, the 2^+ of the γ band decays with considerable strength to the 2_1^+ level, with $B(E2; 2_2^+ \rightarrow 2_1^+) = 42(9)$ W.u. and very little strength to the 0^+ ground state, with $B(E2; 2_2^+ \rightarrow 0_1^+) = 0.90(22)$ W.u. [10]. This is again in good agreement with the SM predictions of $B(E2; 2_2^+ \rightarrow 2_1^+) = 33$ W.u. and $B(E2; 2_2^+ \rightarrow 0_1^+) = 1.5$ W.u. Thus, the SM calculations can reproduce both the energy spacings as well as the overall collectivity of the γ band. In addition, the $B(E2)$ ratios R_{SM} are found to be in good agreement with the data for all but the 6^+ level (see Table II). While the collective DF model points to a rigid triaxial shape for ^{76}Ge , the corresponding

excellent agreement with SM calculations shows that such behavior can be generated from a microscopic basis. Note that the SM calculations of Ref. [27] correctly reproduce the γ -soft staggering pattern exhibited in $^{78,80}\text{Se}$ while predicting a γ -rigid staggering pattern in the γ band of ^{78}Ge , similar to that observed in ^{76}Ge . This suggests a possible region of triaxiality rather than an isolated instance. Extending these measurements to more neutron-rich Ge isotopes would test the SM predictions and potentially shed more light on the microscopic underpinnings to rigid triaxial shapes.

In conclusion, the level scheme of ^{76}Ge has been improved significantly through measurement of prompt $\gamma\gamma\gamma$ coincidence data from reactions between a ^{76}Ge beam and a ^{238}U target with the Gammasphere detector array. The γ band has now been identified up to the 9^+ state. This work constitutes the first determination of the staggering in a γ band above $I = 4$ for the $A \geq 70$ Ge isotopes. Analysis of the staggering pattern in the γ band of ^{76}Ge finds a phase consistent with the predictions for a rigid-triaxial shape, although the amplitude is considerably less than the collective-model predictions. Comparison of staggering patterns in neighboring isotopes finds this is a unique occurrence in this region and, in fact, is a rarity across the nuclear chart. Shell-model calculations of ^{76}Ge reproduce both the phase and the magnitude of the γ -band staggering.

The authors thank the ATLAS operating staff for the efficient running of the accelerator, and Drs. M. Sugawara, M. Koizumi, and A. O. Macchiavelli for their valuable comments. This work was supported in part by the US Department of Energy, Office of Nuclear Physics, under Contracts No. DE-AC02-06CH11357 and No. DE-AC02-98CH10946 and Grant No. DE-FG02-94-ER40834, and by the Polish Ministry of Science under Contract No. 1P03B05929.

-
- [1] S. W. Ødegård *et al.*, *Phys. Rev. Lett.* **86**, 5866 (2001).
 [2] G. Schönwaßer *et al.*, *Phys. Lett. B* **552**, 9 (2003).
 [3] D. J. Hartley *et al.*, *Phys. Rev. C* **80**, 041304(R) (2009).
 [4] T. Koike, K. Starosta, P. Joshi, G. Rainovski, J. Timár, C. Vaman, and R. Wadsworth, *J. Phys. G: Nucl. Part. Phys.* **31**, S1741 (2005).
 [5] A. Bohr and B. R. Mottelson, *Kgl. Dan. Vidensk. Selsk. Mat.-Fys. Medd.* **27**, 16 (1953).
 [6] A. S. Davydov and G. F. Filippov, *Nucl. Phys.* **8**, 237 (1958).
 [7] Lawrence Wilets and Maurice Jean, *Phys. Rev.* **102**, 788 (1956).
 [8] N. V. Zamfir and R. F. Casten, *Phys. Lett. B* **260**, 265 (1991).
 [9] D. Abriola and A. A. Sonzogni, *Nucl. Data Sheets* **111**, 1 (2010).
 [10] B. Singh, *Nucl. Data Sheets* **74**, 63 (1995).
 [11] Balraj Singh and Ameenah R. Farhan, *Nucl. Data Sheets* **107**, 1923 (2006).
 [12] J. K. Tuli, *Nucl. Data Sheets* **103**, 389 (2004).
 [13] W.-T. Chou, D. S. Brenner, R. F. Casten, and R. L. Gill, *Phys. Rev. C* **47**, 157 (1993).
 [14] W. Andrejtscheff and P. Petkov, *Phys. Lett. B* **329**, 1 (1994).
 [15] Lu Guo, J. A. Maruhn, and P.-G. Reinhard, *Phys. Rev. C* **76**, 034317 (2007).
 [16] I-Yang Lee, *Nucl. Phys. A* **520**, 641c (1990).
 [17] P. J. Nolan, F. A. Beck, and D. B. Fossan, *Annu. Rev. Nucl. Part. Sci.* **44**, 561 (1994).
 [18] N. Hoteling *et al.*, *Phys. Rev. C* **74**, 064313 (2006).
 [19] D. C. Radford, *Nucl. Instrum. Methods Phys. Res. A* **361**, 297 (1995).
 [20] Zs. Podolyak *et al.*, *Int. J. Mod. Phys. E* **13**, 123 (2004).
 [21] S. Mordechai, H. T. Fortune, R. Middleton, and G. Stephans, *Phys. Rev. C* **18**, 2498 (1978).
 [22] David C. Camp and Bruce P. Foster, *Nucl. Phys. A* **177**, 401 (1971).
 [23] B. Ramstein, R. Tamisier, L. H. Rosier, P. Avignon, and J. P. Delaroche, *Nucl. Phys. A* **411**, 231 (1983).
 [24] E. A. McCutchan, D. Bonatsos, N. V. Zamfir, and R. F. Casten, *Phys. Rev. C* **76**, 024306 (2007).
 [25] C. Mihai *et al.*, *Phys. Rev. C* **75**, 044302 (2007). Note that a minus sign was omitted from the values of $S(4)$ given for $^{78,80,82}\text{Se}$.
 [26] E. Bouchez *et al.*, *Phys. Rev. Lett.* **90**, 082502 (2003).
 [27] N. Yoshinaga, K. Higashiyama, and P. H. Regan, *Phys. Rev. C* **78**, 044320 (2008).